On one Stefan-type problem for the objects with complex geometry

V.I.Zubov*, A.F.Albu†
*Вычислительный центр РАН, zubov@ccas.ru
† Вычислительный центр РАН, albou@ccas.ru

Abstract

The optimal control problem of metal solidification in casting is considered. The process is modeled by a three-dimensional two-phase initial–boundary value problem of the Stefan type. The direct problem was solved for an actual object with complex geometry. The optimal control problem was solved numerically using the gradient method.

Introduction

Stefan problems form an important class of heat transfer problems. A key feature of these problems is that they involve a moving interface between two phases (liquid and solid). The law of motion of the interface is unknown in advance and is to be determined. The thermal properties of the substance on the different sides of the moving interface can be different. We consider an important and interesting problem of this class, namely, the optimal control of the process of solidification in metal casting. The cooling of liquid metal in the furnace proceeds as follows. On the one hand, the mold is slowly immersed in the low-temperature liquid aluminum, which causes the solidification of the metal. On the other hand, the mold gains heat from the walls of the furnace, which prevents the solidification process from proceeding too fast.

The optimal control problem is to choose a regime of metal cooling and solidification at which the solidification front has a preset shape (or is close to it) and moves sufficiently slow (at a speed close to the preset one).

The formulated optimal control problem was solved numerically. The control was approximated by a piecewise constant function. A different number of intervals on which the function is constant were used. The gradient method was chosen for the minimization of the cost functional.

1. Mathematical formulation of the problem

The following optimal control problem of metal solidification in casting is considered.

A mold with specified outer and inner boundaries is filled with liquid metal (the longitudinal projections of an actual mold are presented in fig. 1). The hatched area in the fig. 1 depicts the mold wall, and the internal unhatched area shows the inside space filled with liquid metal. The mold and the metal inside it are heated up to prescribed temperatures T_{form} and T_{met}, respectively. Next, the mold filled with metal (which is hereafter referred to as the object) begins to cool gradually under varying surrounding conditions. The different parts of the mold's outer boundary are under different thermal conditions (i.e. the laws of heat transfer with the surroundings are different in these parts). Moreover, the thermal conditions affecting the parts vary with time.

The process of cooling the metal and the mold is described by a three-dimensional unsteady heat equation

$$\rho C \frac{\partial T}{\partial t} = div(K \cdot \nabla T), \quad (x, y, z) \in Q. \quad (1)$$

Here x, y, and z are the Cartesian coordinates of a spatial point; t is time; Q is a domain with a piecewise smooth boundary Γ; $T(x, y, z, t)$ is the substance temperature at the point with coordinates (x, y, z) at time t; ρC, and K are the density, heat capacity, and thermal conductivity of the substance, respectively.

The conditions of heat transfer with the surrounding medium are set on the boundary Γ of Q. These conditions depend on the given surface point and time. However, all the heat transfer conditions can be written in the general form:

$$\tilde{\alpha} T + \tilde{\beta} \frac{\partial T}{\partial n} = \tilde{\gamma}. \quad (2)$$

Here $\tilde{\alpha}$, $\tilde{\beta}$, and $\tilde{\gamma}$ are given functions of the coordinates (x, y, z) of a point on Γ and the temperature $T(x, y, z, t)$ and $\frac{\partial T}{\partial n} = T_n$ is the derivative of T in the direction n on the external normal to the surface Γ. It should be noted that the coefficients ρC, and K in (1) and (2) are different for the metal and the mold. They have the form:

$$K(T) = \begin{cases} K_1(T), & (x, y, z) \in metal, \\ K_2(T), & (x, y, z) \in mold, \end{cases}$$

$$K_1(T)=\begin{cases}k_S, & T<T_1,\\ \dfrac{k_L-k_S}{T_2-T_1}T+\dfrac{k_ST_2-k_LT_1}{T_2-T_1}, & T_1\le T<T_2\\ k_L, & T\ge T_2,\end{cases}$$

$$K_2(T)=\begin{cases}k_{\Phi_1}, & T\le T_3,\\ k_{\Phi_2}, & T_3<T,\end{cases}$$

$$\rho(T)=\begin{cases}\rho_1(T), & (x,y,z)\in metal,\\ \rho_\Phi, & (x,y,z)\in mold,\end{cases}$$

$$\rho_1(T)=\begin{cases}\rho_S, & T<T_1,\\ \rho_L, & T\ge T_2,\end{cases}$$

$$C(T)=\begin{cases}C_1(T), & (x,y,z)\in metal,\\ c_\Phi, & (x,y,z)\in mold,\end{cases}$$

$$C_1(T)=\begin{cases}c_S, & T<T_1,\\ c_L, & T\ge T_2.\end{cases}$$

The constants c_S, c_L, c_Φ, ρ_S, ρ_L, ρ_Φ, k_S, k_L, k_{Φ_1}, k_{Φ_2}, T_1, T_2, and T_3 are assumed to be known.

It should be noted that the thermodynamic coefficients have a jump at the metal–mold interface. Two conditions are set at this surface, namely, the temperature and the heat flux must be continuous. Note also that the metal can be simultaneously in two phases: solid and liquid. The domain separating the phases is determined by a narrow range of temperatures $[T_1,T_2]$, in which ρC, and K change very rapidly.

Thus, the solution to the direct problem consists in determining a function $T(x,y,z,t)$ that satisfies eq. (1) in Q, conditions (2) on the outer boundary Γ of Q, and the continuity conditions for the temperature and the heat flux at the metal–mold interface.

The basic types of thermal conditions at a point on the outer boundary of the body can be described as follows.

1) If the point is in the liquid aluminum, the following processes have to be taken into account:
(i) the heat lost by the body due to its own radiation;
(ii) the heat gained from the surrounding liquid aluminum due to its radiation;
(iii) the heat transfer due to conduction between the liquid aluminum and the body.

2) If the point is outside the liquid aluminum, the following processes have to be taken into account:
(i) the heat lost by the body due to its own radiation;
(ii) the heat gained from the emitting walls of the furnace;
(iii) the heat gained from the emitting surface of the liquid aluminum.

The optimal control problem is to choose a regime of metal cooling and solidification at which the solidification front has a preset shape or is close to it (namely, a plane orthogonal to the vertical axis of the object) and moves sufficiently slow (at a speed close to the preset one). The evolution of the solidification front is affected by numerous parameters (for example, by the furnace temperature, the liquid aluminum temperature, the depth to which the object is immersed in the liquid aluminum, the speed at which the mold moves relative to the furnace, etc.). The solidification front as a function of the velocity of the object is of special interest in practice.

The speed $U(t)$ of the displacement of foundry mold in the melting furnace was chosen as the control. The cost function is next:

$$I(U)=\frac{1}{(t_2-t_1)}\int_{t_1}^{t_2}\iint_S\left[Z_{pl}(x,y,t)-z_*(t)\right]^2 dxdy\,dt\,. \quad (3)$$

Here t_1 is the moment, when the crystallization front is conceived; t_2 is the moment, when the crystallization of metal completes; $(x,y,Z_{pl}(x,y,t))$ are the real coordinates of the interface at the moment t; $(x,y,z_*(t))$ are the desired coordinates of the interface at the moment t; S is the cross section of the mold that is filled by metal. The control function may be restricted by some prescribed functions $U_1(t)$ and $U_2(t)$: $U_1(t)\le U(t)\le U_2(t)$.

2. The solving of the direct problem

The object being investigated is approximated by the body, which consists of a finite number of rectangular parallelepipeds. The approximating body is placed wholly into a certain large parallelepiped. In this large parallelepiped a basic non-uniform rectangular grid is introduced in such a way, that all external surfaces of the approximating body, and also surfaces, which divide metal and form, would coincide with the grid surfaces. Besides the basic grid, the auxiliary grid is built, whose surfaces are parallel to the surfaces of the basic grid and are displaced relative to it with a half-step in all directions. As a result this entire object being investigated is broken by the surfaces of auxiliary grid to the elementary volumes.

Formulated direct problem is approximated on the constructed grid. For each elementary volume the equation of heat balance is written in the terms of enthalpy (see [1], [2]). In connection with this the concept of

summary enthalpy, which considers the volume fraction of metal and the volume fraction of the form in each volume element, is introduced [2]. The field of temperature in the metal and in the mould is instituted numerically with usage of the Peaceman-Rachford scheme [3] and of the method proposed in [4]. At each moment the segregation of the surface between liquid and solid metal was carried out.

The direct problem was solved for an actual object. Its longitudinal projections are displayed in fig. 1. This object had two planes of symmetry and was located symmetrically in the furnace. It consisted of five parallelepipeds. The exterior view of its quarter is shown in fig. 2. The object was immersed into the molten aluminum up to the fourth parallelepiped. The speed $U(t)$ of the displacement of foundry mold was set equal to zero, when it reached the maximum permissible depth.

The numerical results presented below were obtained for this object and for the real parameter values.

In the computation of the direct problem, primary attention was given to the evolution of the solidification front. The solidification front as a function of the velocity is illustrated in figures 3–10, which show lines of constant temperature at different times in two cross sections ((a) and (b)) through the object's vertical axis of symmetry parallel to the object faces. Since the object is symmetric about the vertical axis, the figures present only halves of the cross sections. The light vertical and horizontal lines inside the parallelepiped separate the metal and the mold. The light curves show lines of constant temperature, and the heavy curve depicts the contour line of $T = T_{pl}$. It separates the liquid and solid phases in the metal. The figures with different numbers correspond to different times.

Figures 3–6 (first experiment) illustrate the process of metal solidification in a mold moving relative to the furnace at the constant speed $U(t) = 2$ mm/min. In the second experiment (figures 7–10), the speed was piecewise constant. More specifically, it remained constant in three time intervals. Over the first time interval, the first (narrowest) parallelepiped was immersed in the coolant at the speed 20 mm/min. Over the second and third time intervals, the second and third parallelepipeds were immersed into the coolant at the speeds 10 and 5 mm/min respectively. Poor results were obtained when the object moved at a constant low speed. The solidification of the metal proceeded from two sides (lower and upper). This led to the formation of bubbles of liquid metal that collapse inside the casting. It should be noted that the solidification front was nearly always far from a horizontal plane. In the second experiment, the solidification front always intersected the metal transversally only once and was noticeably more similar to a horizontal plane. No bubbles of liquid metal were observed inside the casting during the entire process.

3. The results of solving the optimal control problem

During the solution of the optimal control problem the time interval $[0, t^J]$ was divided into N parts (subintervals). The control function $U(t)$ was approximated by piecewise constant function, so that for each of subintervals it was constant. The cost functional $I(U)$ was approximated by function $J(U)$ with the aid of the trapezoid method. The coordinates of the solidification front $\left(x, y, Z_{pl}(x, y, t)\right)$ at the moment t^j were defined by a linear interpolation of the temperature field, obtained as the solution of the direct problem, analogous to how this was done in the work [5].

The formulated optimal control problem was solved numerically using the gradient method. For calculating the objective function $J(U)$ the direct problem was solved on each iteration. The gradient of the cost functional on each iteration was determined with the aid of the finite-difference method. The value ΔU_k of the increase of component k of the control was selected from the requirement of accuracy.

The optimal control problem was studied for a rectangular parallelepiped. The parallelepiped was immersed into the liquid aluminum to 5/6 of its height. Z-coordinate $z_*(t)$ of the desired solidification front changed with a constant velocity $U_*(t) = 0.1$ mm/s. Calculations were performed for different numbers N of subintervals, on which the control function $U(t)$ was constant.

On the fig. 11(a) the dependence of the optimal cost functional $J(U)$ from the number N of subintervals is represented. It is obtained as the result of the solution of optimization problem. Here N has the following values: 1, 2, 4, 12, 24, 600. As shown on fig. 11(a), the optimal value of the functional decreases noticeably for the small values of N, and for the great values of N ($N > 30$) it weakly diminishes and comes out to a certain constant asymptotical value. The fig. 11(b) is a fragment of the fig. 11(a) on which there is no point corresponding to the value $N = 600$. This makes it possible to examine more precisely the dependence of the optimal value of the cost functional from the number of subintervals at low values of N.

On figures 12 the optimal trajectories of the foundry mold are shown. These are those trajectories, with which are obtained optimum values of functional examined above (see fig. 11), namely, for $N = 1, 2, 4, 12, 24, 600$. Numbers near the curves indicate the number N of subintervals used. The convergence of the optimal trajectories to a certain

limit function when the number N increase is visible on figures 12. Let us note that the qualitatively correct structure of optimal trajectory is already obtained for $N=12$. Further increase of the number N only smoothes the optimal trajectory.

Figure 13 shows the behavior of the standard deviation of the real solidification front from the desired one for several control functions. Standard deviation is determined by the formula

$$D(t)=\sqrt{\frac{1}{|S|}\iint_S\left[Z_{pl}(x,y,t)-z_*(t)\right]^2 dxdy}\,, \tag{20}$$

where S is the cross section of the parallelepiped, and $|S|$ is its area. Curve 1 on fig. 13 corresponds to the regime, when the foundry mold is moved with a small constant velocity $U(t)=0.083$ mm/s relatively to the furnace. Curve 2, just as curve 1, corresponds to the regime with a constant velocity of the displacement of the foundry mold, but $U(t)=0.150$ mm/s. Curve 3 corresponds to such displacement of foundry mold, when the functional (3) reaches the minimum value. Figure 14 represents the control functions that correspond to the regimes indicated. All these calculations were performed for $N=24$.

Figure 15 illustrates the dependence of the standard deviation $D(t)$ of the real solidification front (found as the result of the solution of optimization problem) from the desired one, upon the number N. Numbers near the curves indicate the number of subintervals N used. Figure 15 shows the convergence of the function $D(t)$ to a certain limit function with the increase of the number N. Let us note that for $N>15$ the curves $D(t)$ almost coincide with the curve obtained for $N=24$ and therefore they are not represented on fig. 15.

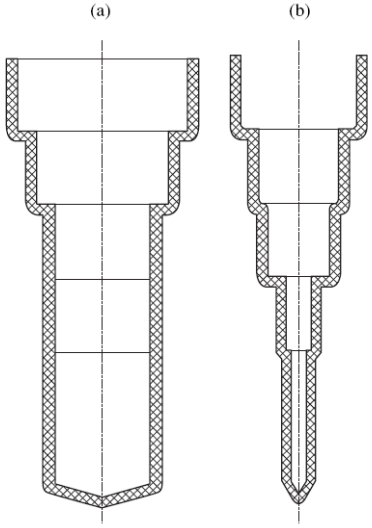

Fig. 1

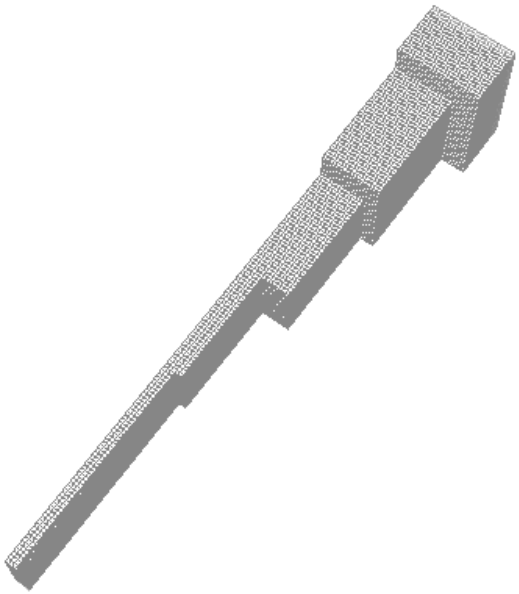

Fig. 2

References

1. White R. E., 1982, An enthalpy formulation of the Stephan problem. SIAM J. Numer. Anal., **19**, 1129–1157.

2. Albu A. F. and Zubov V. I., 2007, Mathematical Modeling and Study of the Process of Solidification in Metal Casting. Zh. Vychisl. Mat. Mat. Fiz. **47**, 882–902 (2007).

3. Samarskii A. A., 2001, The Theory of Difference Schemes (New York: Marcel Dekker).

4. Albu A. F. and Zubov V. I., 2001, A modified scheme for analyzing the process of melting. Comp. math. math. phys., **41**, 1363–1371.

5. Albu A. F., Gorbunov V. I. and Zubov V. I., 2000, Optimal control of the process of melting. Comp. math. math. phys., **40**, 491–504.

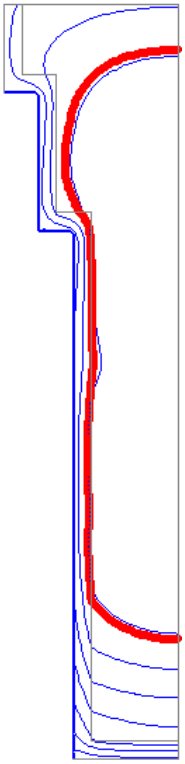

Fig. 3a

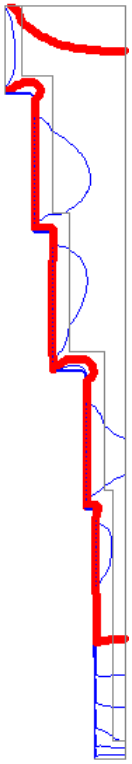

Fig. 3b

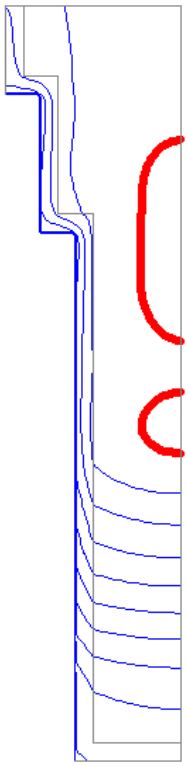

Fig. 5a

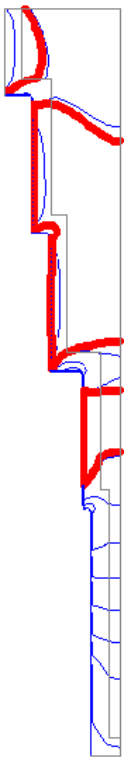

Fig. 5b

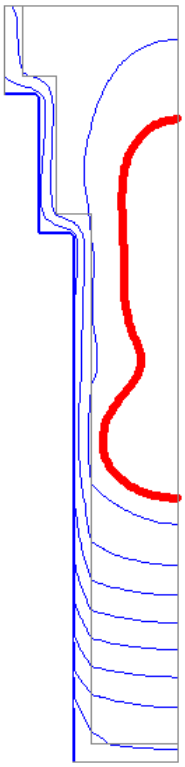

Fig. 4a

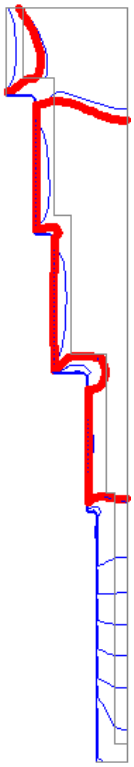

Fig. 4b

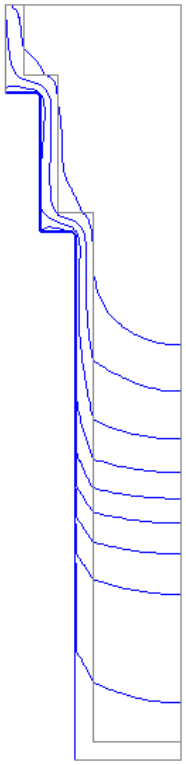

Fig. 6a

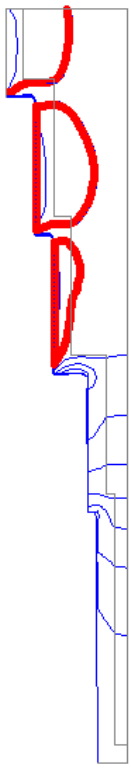

Fig. 6b

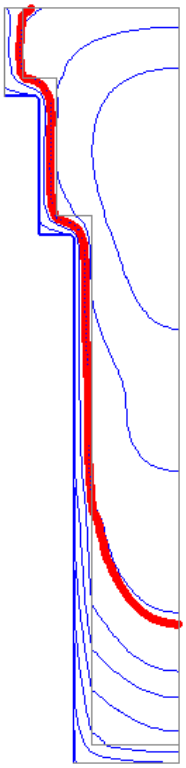

Fig. 7a

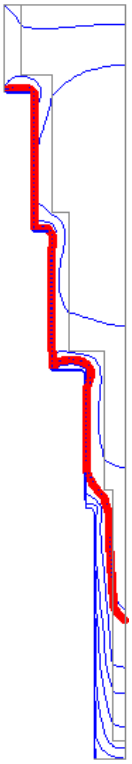

Fig. 7b

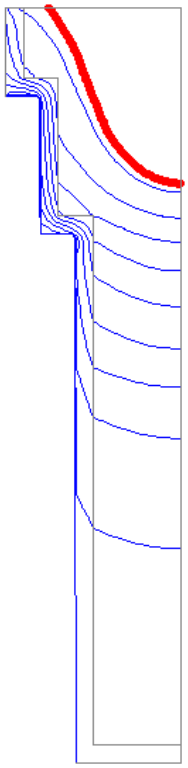

Fig. 9a

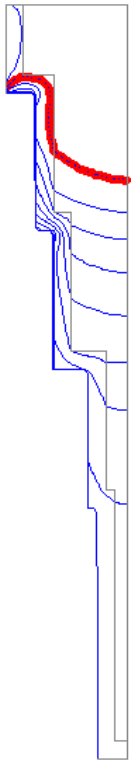

Fig. 9b

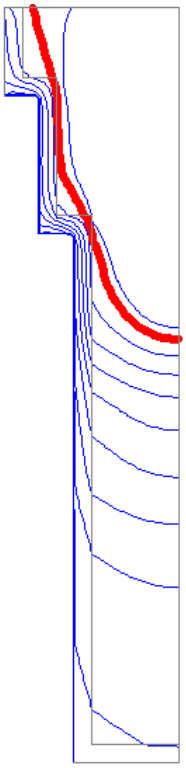

Fig. 8a

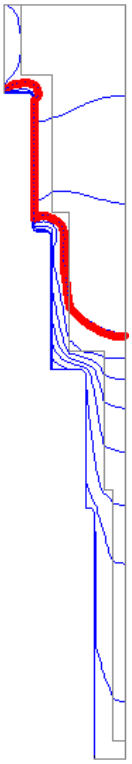

Fig. 8b

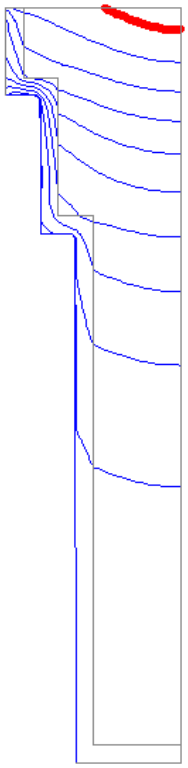

Fig. 10a

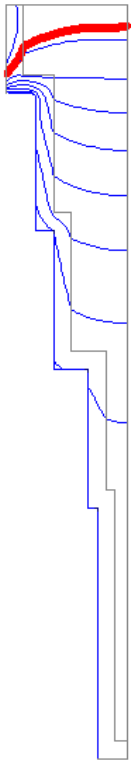

Fig. 10b

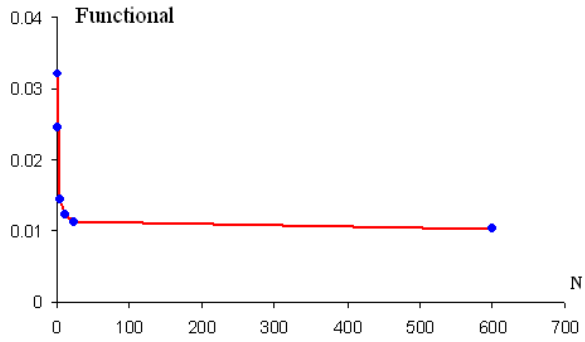

Fig. 11a

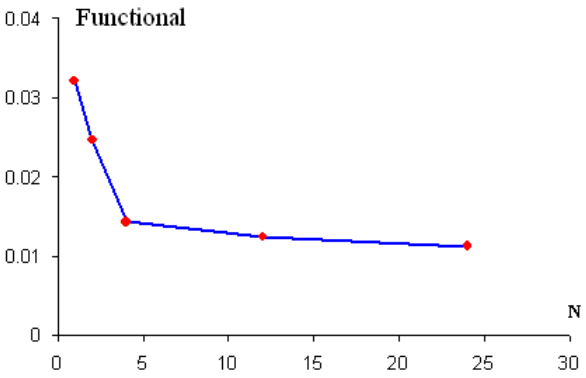

Fig. 11b

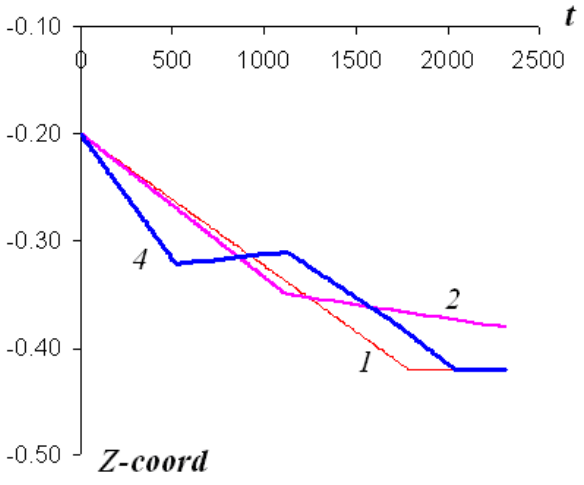

Fig. 12a

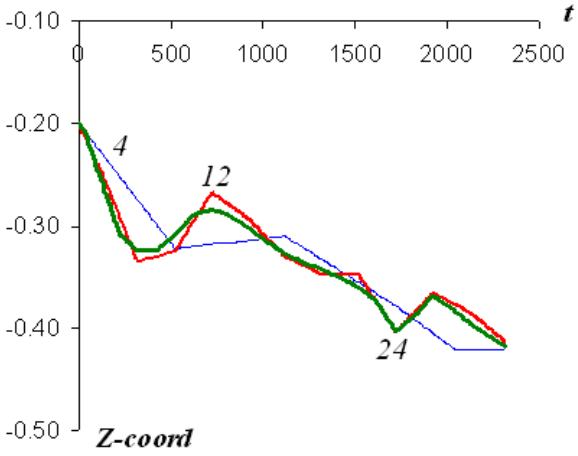

Fig. 12b

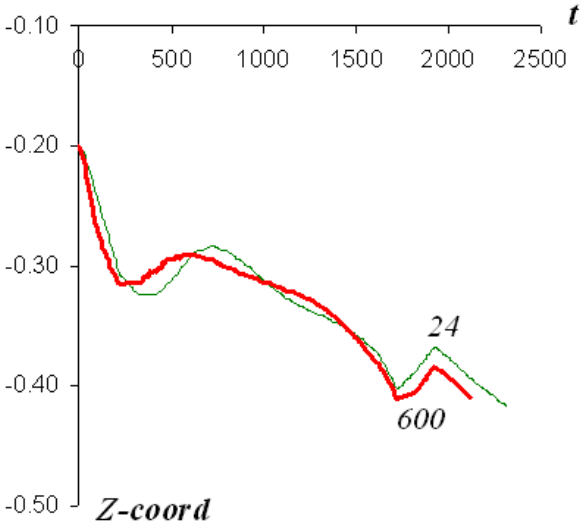

Fig. 12c

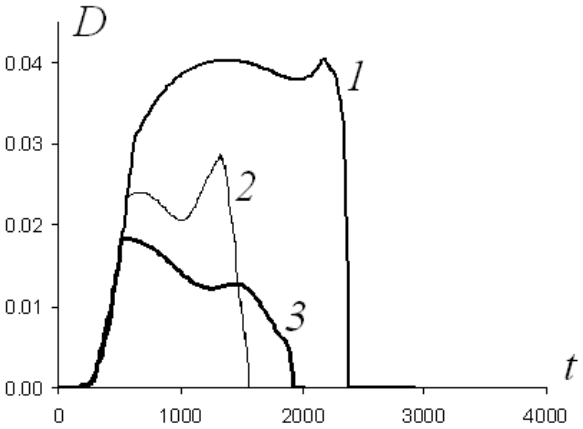

Fig. 13

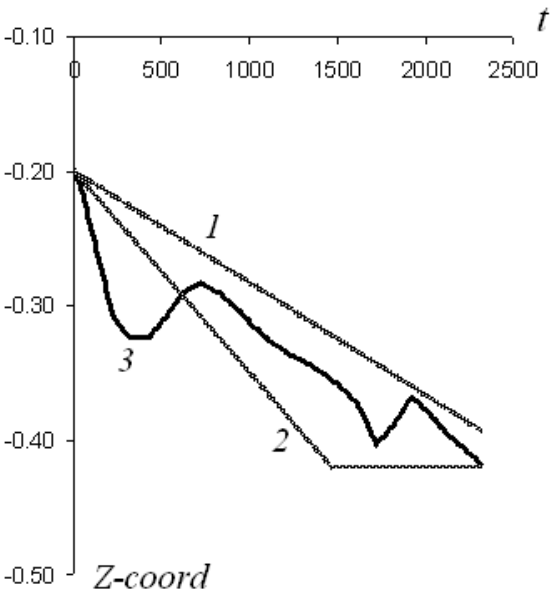

Fig. 14

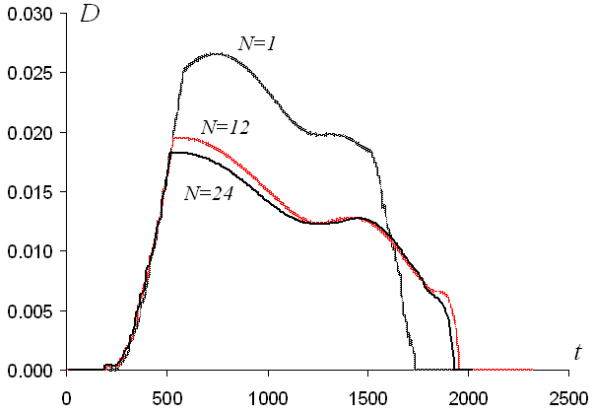

Fig. 15

Acknowledgments

This work was supported by the Russian Foundation for Basic Research (project no. 05-01-00063) and the program “Leading Scientific Schools” (project no. NSh-2240.2006.1).